CHEMICAL COMMUNICATIONS

The importance of methylation in the binding of (ferrocenylmethyl)-tempammonium guests by cucurbit[*n*]uril (*n* = 7, 8) hosts

Song Yi, Burjor Captain and Angel E. Kaifer*

Center for Supramolecular Science and Department of Chemistry

University of Miami, Coral Gables, Florida 33124-0431, USA

ELECTRONIC SUPPORTING INFORMATION

Materials

CB7 and CB8 were prepared following a reported procedure.[1] 4-amino-TEMPO, 4-oxo-TEMPO, ferrocenecarboxaldehyde and sodium hydrosulfite were purchased from Sigma-Aldrich and used without further purification.

Preparation of coumpound **1**: To a stirred absolute methanol solution (50 mL) of ferrocenecarboxaldehyde (200 mg, 0.93 mmol) and 4-amino-TEMPO (960 mg, 5.6 mmol) with activated 4A type molecular sieves was added 5 M HCl in MeOH to adjust the pH of the solution to ca. 7. After stirring for 1 h at r.t. under N_2, $NaBH_3CN$ (352 mg, 5.6 mmol) was added to the reaction mixture which was then heated and stirred at 60°C for 2 days. The resulting mixture was filtered through Celite 545 and then concentrated in vacuo to give a red solid, which was purified by column chromatography on Al_2O_3 (neutral) by using mixed solvent of *n*-hexane and ethyl acetate (10:1) as eluent. The final product was obtained as pale orange rods (288 mg, yield: 83.5%) after the solvent was evaporated and recrystallized from acetonitrile. ESI-HRMS (m/z) calcd for $C_{20}H_{29}N_2OFe$: 370.1702, found: 370.1710; elemental analysis calcd (%) for $C_{20}H_{29}N_2OFe$: C 65.01, H 7.92, N 7.59; found: C 65.19, H 7.89, N 7.56.

Preparation of compound **2**: 4-Methylamino-TEMPO was prepared according to a reported procedure.[2] Compound **2** was synthesized following a procedure similar to that for compound **1**, in which 4-methylamino-TEMPO was used instead of 4-amino-TEMPO. The final product was obtained as orange needles by recrystallization form *n*-hexane or acetonitrile, yield: 70.6%. ESI-HRMS (m/z) calcd for $C_{21}H_{31}N_2OFe$: 384.1859, found: 384.1865; elemental analysis calcd (%) for $C_{21}H_{31}N_2OFe$: C 65.77, H 8.15, N 7.31; found: C 65.74, H 8.15, N 7.28.

Preparation of compound **3**: Compound **2** (100 mg, 0.26 mmol) was dissolved in 10 mL acetonitrile, and then methyl iodide (1 mL, 16.0 mmol) was added. After stirring for 5 h at r.t., the reaction mixture was concentrated in vacuo to give a red solid. The final product was obtained as orange rods (105 mg, yield: 76.6%) crystallized from a mixed solvent (methanol and diethyl ether). ESI-HRMS (m/z) calcd for $C_{22}H_{34}N_2OFe$: 398.2021, found: 398.2018; elemental analysis calcd (%) for $C_{22}H_{34}N_2OFeI$: C 50.28, H 6.53, N 5.33; found: C 49.68, H 6.63, N 5.59. The product was converted to its

hexafluorophosphate salt by treatment with excess NH_4PF_6. Elemental analysis calcd (%) for $C_{22}H_{34}N_2OFePF_6$: C 48.60, H 6.31, N 5.16; found: C 48.05, H 6.24, N 5.15.

Spectroscopic Experiments

^{1}H NMR spectra were recorded on a Bruker (Billerica, MA) Avance 500 MHz NMR spectrometer. Sodium hydrosulfite (1~2 mg) was added to a sample of 600 μL solution before NMR spectrum was recorded. EPR spectra were recorded on a Bruker EMX 200D spectrometer. The instrument was set as follows: microwave power 6.3 mW, modulation amplitude 0.5 G, modulation frequency 100 kHz, scan time 360 s. Electrochemical experiments were performed with a BAS 100 B/W workstation (Bioanalytical Systems, West Lafayette, IN). A platinum disk working electrode, Pt counter electrode and Ag/AgCl reference electrode were utilized in voltammetric experiments. In all the experiments, HCl or DCl was added to adjust pH to 3.5 for compound **1** and **2**.

Crystallographic Analyses

The data crystals were glued onto the end of a thin glass fiber. X-ray intensity data were measured by using a Bruker SMART APEX2 CCD-based diffractometer using Mo Kα radiation (λ = 0.71073 Å).[3] The raw data frames were integrated with the SAINT+ program by using a narrow-frame integration algorithm.[3] Corrections for Lorentz and polarization effects were also applied with SAINT+. An empirical absorption correction based on the multiple measurement of equivalent reflections was applied using the program SADABS. All structures were solved by a combination of direct methods and difference Fourier syntheses, and refined by full-matrix least-squares on F^2, by using the SHELXTL software package.[4] All non-hydrogen atoms were refined with anisotropic displacement parameters unless otherwise stated. Hydrogen atoms were placed in geometrically idealized positions and included as standard riding atoms during the least-squares refinements. Crystal data, data collection parameters, and results of the analyses are listed in Table S1.

Orange single crystals of **1** suitable for x-ray diffraction analyses obtained by evaporation of solvent from an acetonitrile solution at 25 °C, crystallized in the monoclinic crystal system. The systematic absences in the intensity data were consistent with the unique

space groups $P2_1/c$. Atoms C11 and N1 are disordered over two orientations and were refined in the ratio 50 / 50.

Orange single crystals of **2** suitable for X - ray diffraction analyses were obtained by evaporation of solvent from an acetonitrile solution at 25°C, crystallized in the monoclinic crystal system. The systematic absences in the intensity data were consistent with the unique space group $P2_1/c$.

CCDC 815163 and 815164 contain the supplementary crystallographic data for this paper. These data can be obtained free of charge from The Cambridge Crystallographic Data Centre via.www.ccdc.cam.ac.uk/data_request/cif.

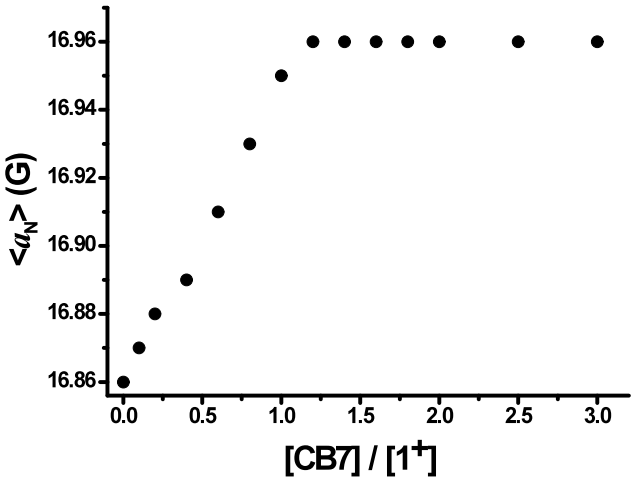

Figure S1. Variation of the hyperfine splitting constant in the EPR spectrum of **1**$^+$ (0.1 mM, pH~3.5) upon addition of CB7.

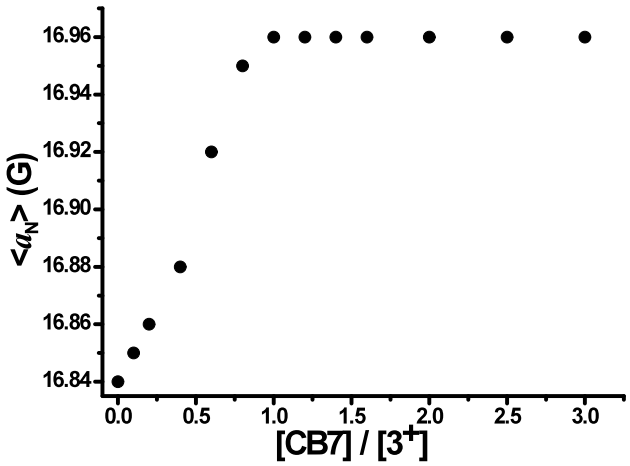

Figure S2. Variation of the hyperfine splitting constant in the EPR spectrum of **3**$^+$ (0.1 mM) upon addition of CB7.

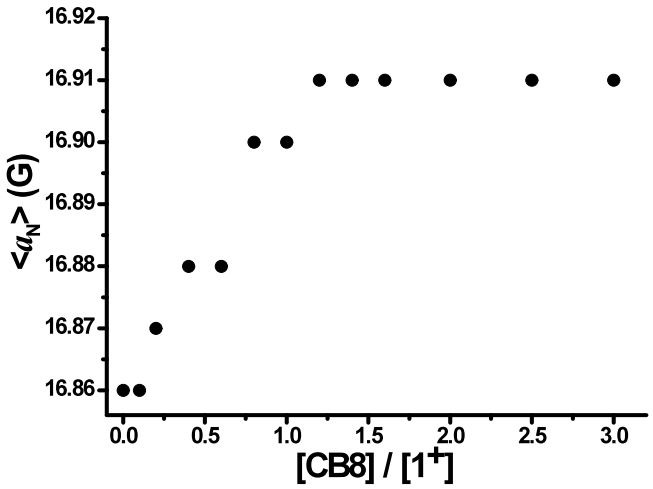

Figure S3. Variation of the hyperfine splitting constant in the EPR spectrum of **1**$^+$ (0.05 mM, pH~3.5) upon addition of CB8.

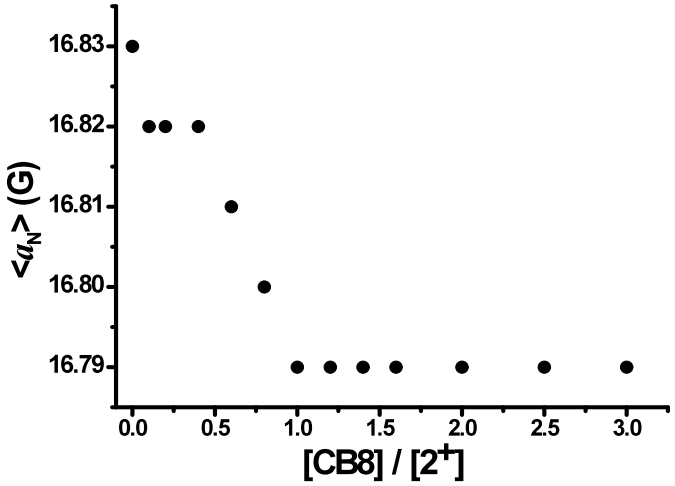

Figure S4. Variation of the hyperfine splitting constant in the EPR spectrum of **2**$^+$ (0.05 mM, pH~3.5) upon addition of CB8.

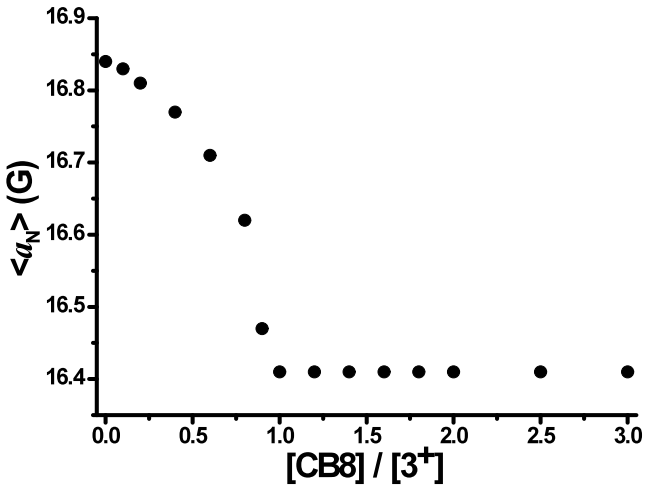

Figure S5. Variation of the hyperfine splitting constant in the EPR spectrum of **3**$^{+}$ (0.05 mM) upon addition of CB8.

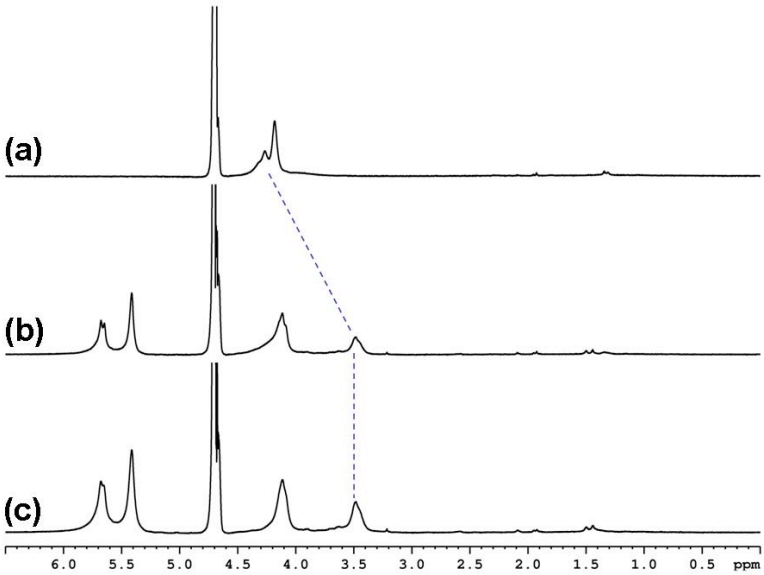

Figure S6. ^{1}H NMR spectra (500 MHz, D_2O/pH*~3.5) of 0.5 mM **1**$^{+}$ in the (a) absence and presence of (b) 0.5 equiv CB7, and (c) 1.0 equiv CB7.

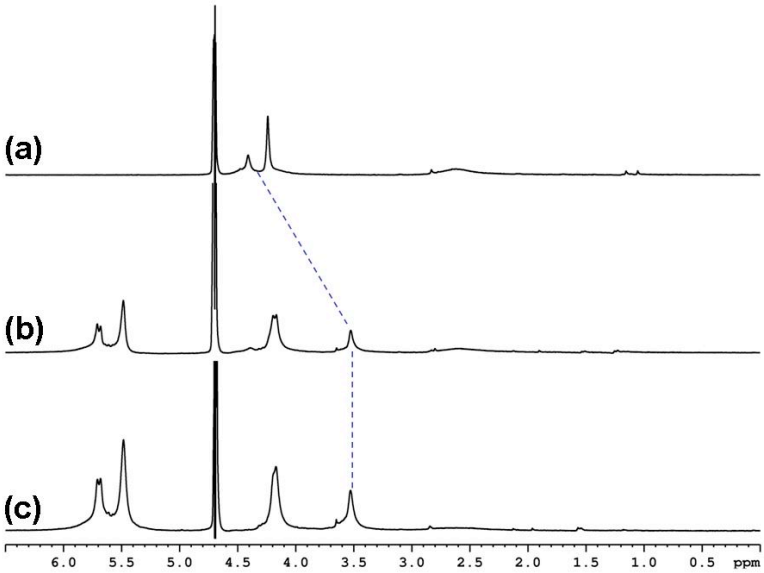

Figure S7. ^{1}H NMR spectra (500 MHz, D_2O) of 0.5 mM **3**$^{+}$ in the (a) absence and presence of (b) 0.5 equiv CB7, and (c) 1.0 equiv CB7.

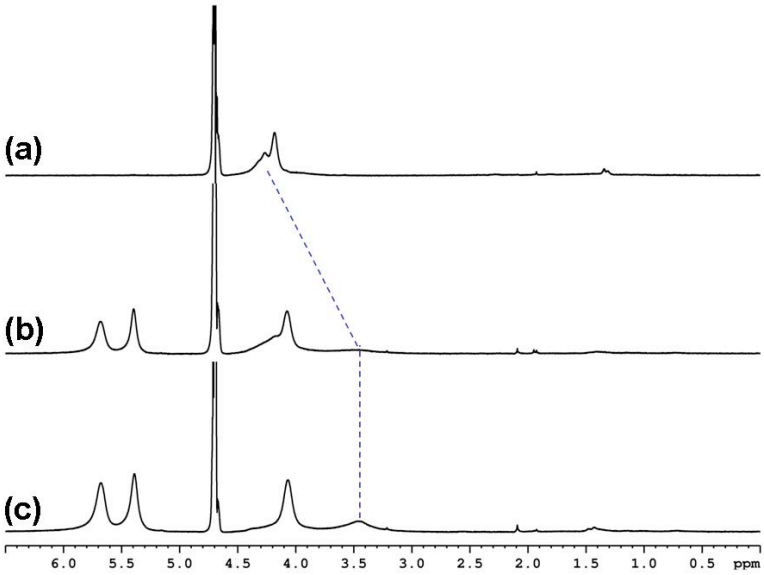

Figure S8. ^{1}H NMR spectra (500 MHz, D_2O/pH*~3.5) of 0.5 mM **1**$^+$ in the (a) absence and presence of (b) 0.5 equiv CB8, and (c) 1.0 equiv CB8.

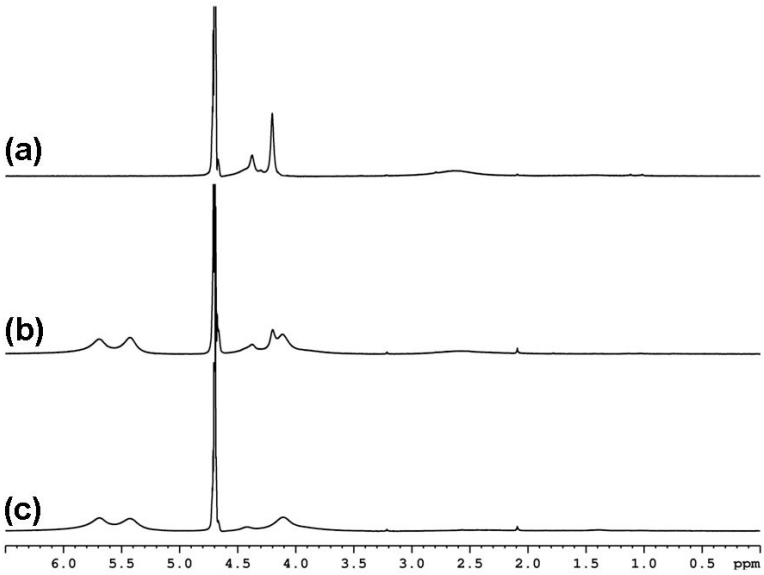

Figure S9. ^{1}H NMR spectra (500 MHz, D_2O) of 0.5 mM **3**$^+$ in the (a) absence and presence of (b) 0.5 equiv CB8, and (c) 1.0 equiv CB8.

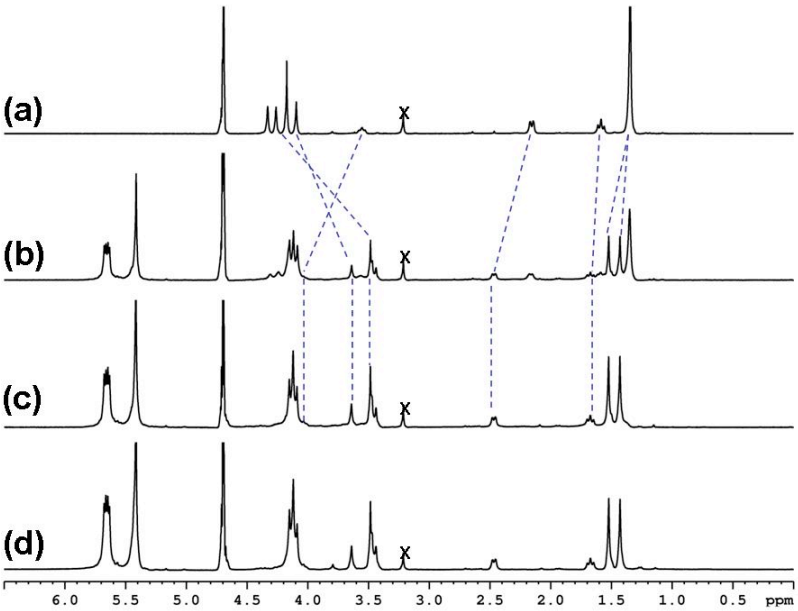

Figure S10. ^{1}H NMR spectra (500 MHz, D_2O/pH*~3.5) of 0.5 mM **1**$^+$ upon reduction with $Na_2S_2O_4$ in the (a) absence and presence of (b) 0.5 equiv CB7, (c) 1.0 equiv CB7, and (d) 1.5 equiv CB7. 'Cross' denotes the impurity from $Na_2S_2O_4$.

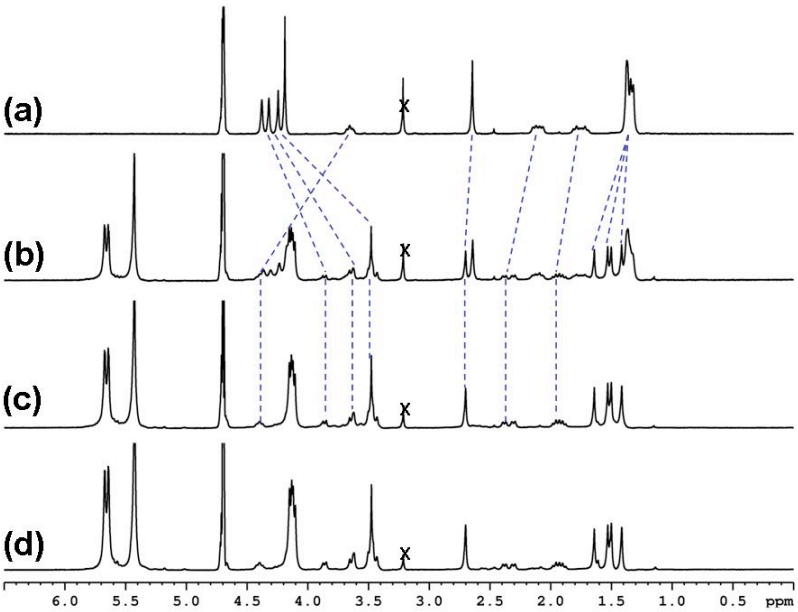

Figure S11. ^{1}H NMR spectra (500 MHz, D_2O/pH*~3.5) of 0.5 mM **2**$^+$ upon reduction with $Na_2S_2O_4$ in the (a) absence and presence of (b) 0.5 equiv CB7, (c) 1.0 equiv CB7, and (d) 1.5 equiv CB7. 'Cross' denotes the impurity from $Na_2S_2O_4$.

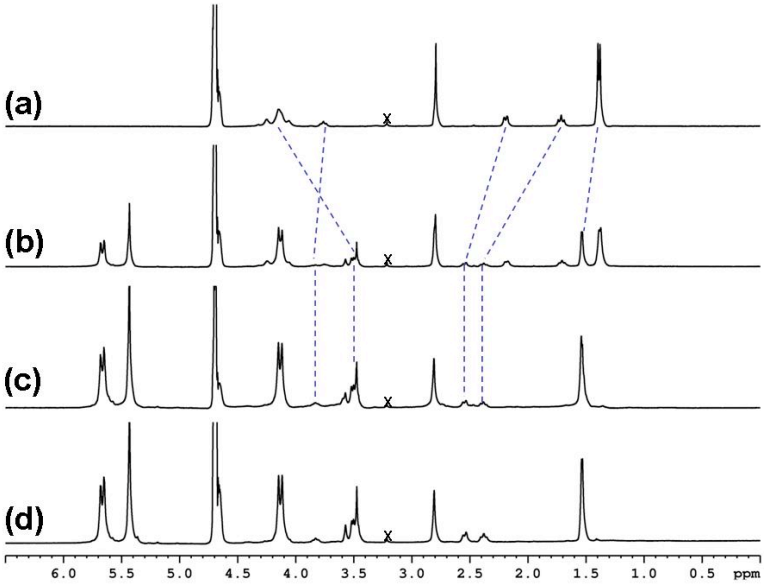

Figure S12. ^{1}H NMR spectra (500 MHz, D_2O) of 0.5 mM **3**$^+$ upon reduction with $Na_2S_2O_4$ in the (a) absence and presence of (b) 0.5 equiv CB7, (c) 1.0 equiv CB7, and (d) 1.2 equiv CB7. 'Cross' denotes the impurity from $Na_2S_2O_4$.

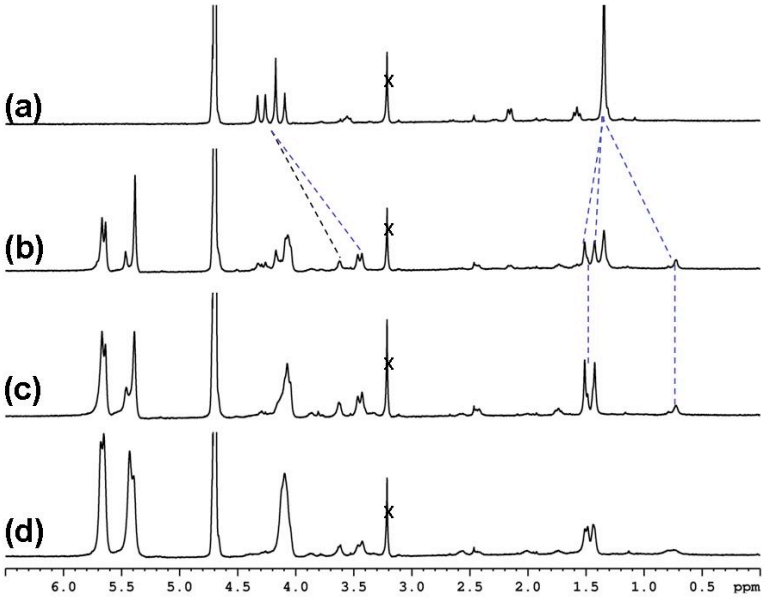

Figure S13. ^{1}H NMR spectra (500 MHz, D_2O/pH*~3.5) of 0.1 mM **1**$^+$ upon reduction with $Na_2S_2O_4$ in the (a) absence and presence of (b) 0.5 equiv CB8, (c) 1.0 equiv CB8, and (d) 1.5 equiv CB8. 'Cross' denotes the impurity from $Na_2S_2O_4$.

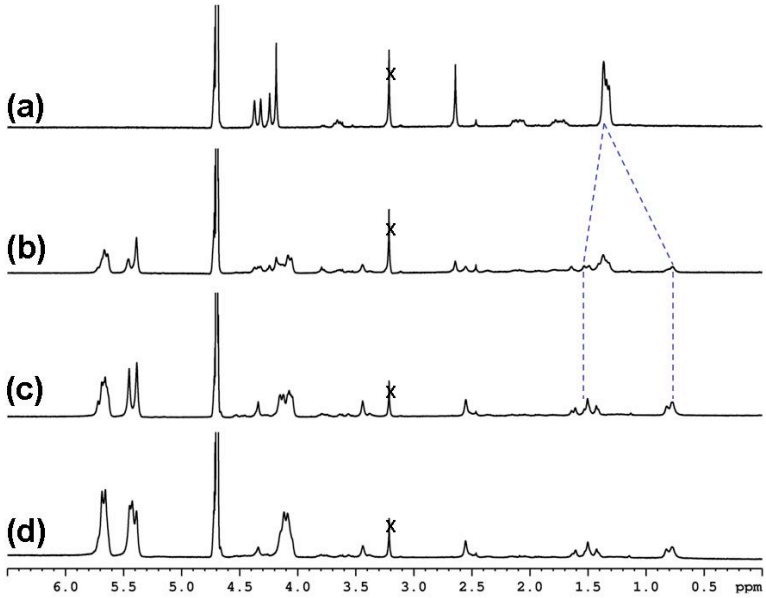

Figure S14. ^{1}H NMR spectra (500 MHz, D_2O/pH*~3.5) of 0.1 mM **2**$^+$ upon reduction with $Na_2S_2O_4$ in the (a) absence and presence of (b) 0.5 equiv CB8, (c) 1.0 equiv CB8, and (d) 1.5 equiv CB8. 'Cross' denotes the impurity from $Na_2S_2O_4$.

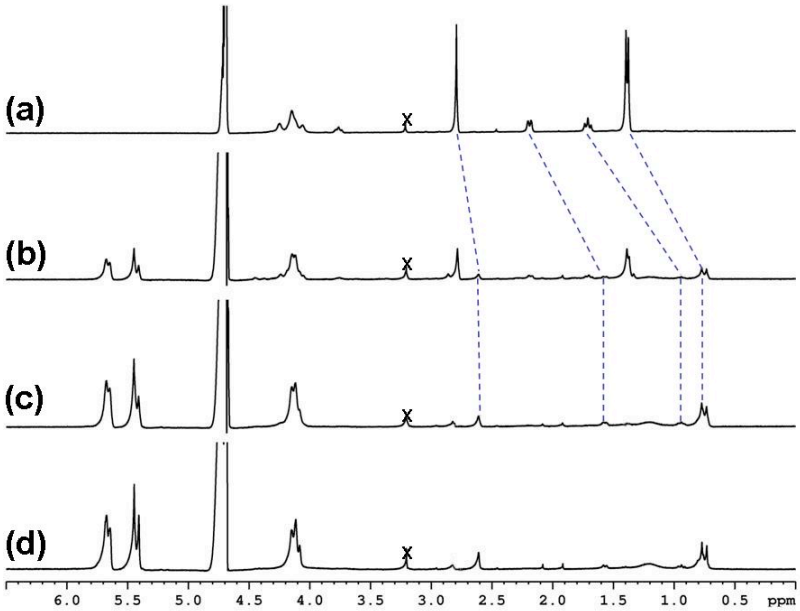

Figure S15. ^{1}H NMR spectra (500 MHz, D_2O) of 0.1 mM **3**$^+$ upon reduction with $Na_2S_2O_4$ in the (a) absence and presence of (b) 0.5 equiv CB8, (c) 1.0 equiv CB8, and (d) 1.5 equiv CB8. 'Cross' denotes the impurity from $Na_2S_2O_4$.

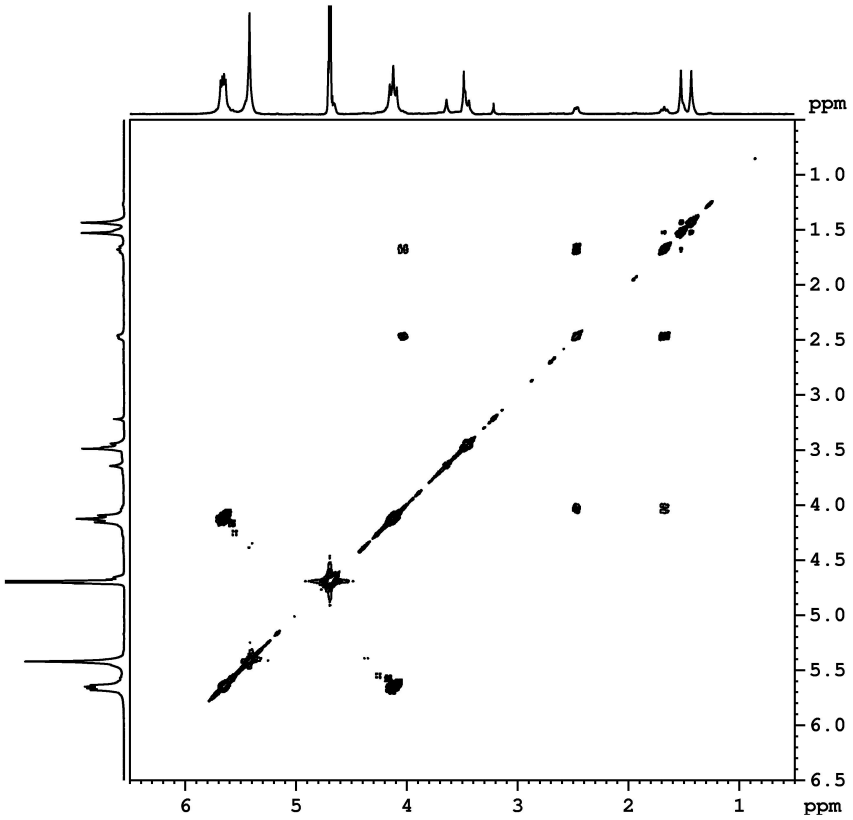

Figure S16. 2D gradient COSY spectrum (500 MHz, D_2O/pH*~3.5) for **1**$^+$ upon reduction with $Na_2S_2O_4$ in the presence of 1.0 equiv CB7.

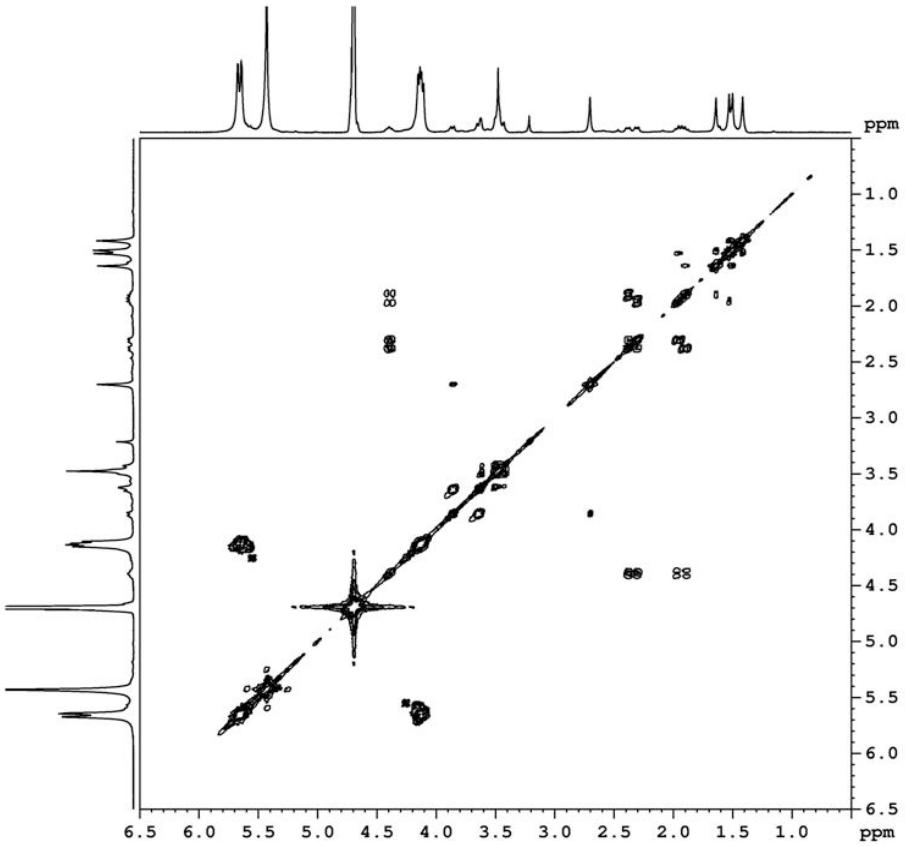

Figure S17. 2D gradient COSY spectrum (500 MHz, D_2O/pH*~3.5) for **2**$^+$ upon reduction with $Na_2S_2O_4$ in the presence of 1.0 equiv CB7.

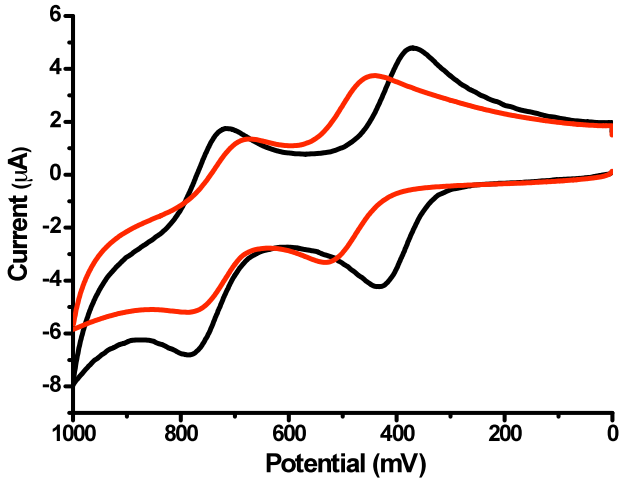

Figure S18. Cyclic voltammetric response of 1.0 mM **1**$^+$ in 50 mM NaCl in the absence (black) and in the presence (red) of 1.0 equiv CB7.

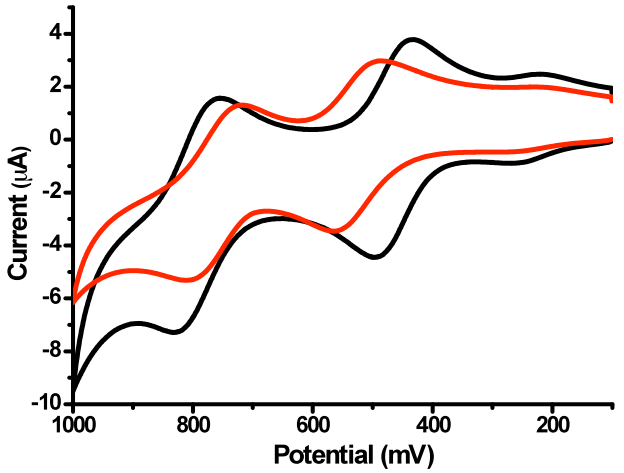

Figure S19. Cyclic voltammetric response of 1.0 mM **3**$^+$ in 50 mM NaCl in the absence (black) and in the presence (red) of 1.0 equiv CB7.

Table S1. Crystallographic Data for Compounds 1 and 2.

	1	**2**
Empirical formula	$FeC_{20}H_{29}N_2O$	$FeC_{21}H_{31}N_2O$
Formula weight	369.30	383.33
Crystal system	Monoclinic	Monoclinic
Lattice parameters		
a (Å)	13.9513(7)	11.6659(5)
b (Å)	5.9462(3)	5.9289(2)
c (Å)	22.6371(11)	28.2755(12)
β (°)	100.1085(7)	99.3020(6)
V (Å^3)	1848.76(16)	1929.98(13)
Space group	$P2_1/c$ (# 14)	$P\,2_1/c$ (# 14)
Z value	4	4
ρ_{calc} (g / cm^3)	1.327	1.319
μ (Mo Kα) (mm^{-1})	0.824	0.792
Temperature (K)	296	296
$2\Theta_{max}$ (°)	54.00	58.0
No. Obs. (I > 2σ(I))	3428	4538
No. Parameters	239	231
Goodness of fit	1.180	1.090
Max. shift in cycle	0.000	0.001
Residuals*:R1; wR2	0.0495; 0.1338	0.0365; 0.0925
Absorption Correction, Max/min	Multi-scan 0.9678/0.7447	Multi-scan 0.9250/0.7023
Largest peak in Final Diff. Map (e$^-$ / Å^3)	0.340	0.495

$*R = \Sigma_{hkl}(\,|\,|F_{obs}| - |F_{calc}|\,|)/\Sigma_{hkl}|F_{obs}|$; $R_w = [\Sigma_{hkl}w(|F_{obs}| - |F_{calc}|)^2/\Sigma_{hkl}wF_{obs}^2]^{1/2}$, $w = 1/\sigma^2(F_{obs})$; $GOF = [\Sigma_{hkl}w(|F_{obs}| - |F_{calc}|)^2/(n_{data} - n_{vari})]^{1/2}$.

References:

[1] Day, A.; Arnold, A. P.; Blanch, R. J.; Snushall, B. *J. Org. Chem.* **2001**, *66*, 8094-8100.

[2] Nakatsuji, S.; Ojima, T.; Akutsu, H.; Yamada, J. *J. Org. Chem.* **2002**, *67*, 916-921.

[3] Apex2 Version 2.2-0 and SAINT+ Version 7.46A; Bruker Analytical X-ray System, Inc., Madison, Wisconsin, USA, 2007.

[4] (a) Sheldrick, G. M. SHELXTL Version 6.1; Bruker Analytical X-ray Systems, Inc., Madison, Wisconsin, USA, 2000. (b) Sheldrick, G. M. *Acta Cryst*. **2008,** *A64*, 112–122.